Electron spin resonance studies of P and B codoped Si nanocrystals

Fujio, Kazuyoshi ; Fujii, Minoru ; Sumida, Kazuaki ; Hayashi, Shinji ; Fujisawa, Masashi ; Ohta, Hitoshi

(Citation)
Applied Physics Letters,93(2):021920-021920

(Issue Date)
2008-07

(Resource Type)
journal article

(Version)
Version of Record

Electron spin resonance studies of P and B codoped Si nanocrystals

Kazuyoshi Fujio,[1] Minoru Fujii,[1,a)] Kazuaki Sumida,[1] Shinji Hayashi,[1] Masashi Fujisawa,[2] and Hitoshi Ohta[3]
[1]*Department of Electrical and Electronic Engineering, Graduate School of Engineering, Kobe University, Rokkodai, Nada, Kobe 657-8501, Japan*
[2]*Department of Frontier Research and Technology, Kobe University, Rokkodai, Nada, Kobe 657-8501, Japan*
[3]*Molecular Photoscience Research Center, Department of Frontier Research and Technology, Headquarters for Innovative Cooperation and Development, Kobe University, Rokkodai, Nada, Kobe 657-8501, Japan*

(Received 5 June 2008; accepted 23 June 2008; published online 18 July 2008)

P- and/or B-doped Si nanocrystals (Si-ncs) embedded in glass matrices were studied by electron spin resonance (ESR) spectroscopy to investigate the origin of strong room-temperature photoluminescence (PL) of *n*- and *p*-type impurities codoped Si-ncs below the band-gap energy of bulk Si crystals. It was shown that the intensity and width of the ESR signal depend strongly on impurity concentrations. A clear correlation was observed between the ESR signal width and the PL intensity. The observed correlation suggests that in addition to the geometrical confinement, P and B codoping further localize carriers in Si-ncs, and the strong localization results in the characteristic luminescence properties. © *2008 American Institute of Physics*. [DOI: 10.1063/1.2957975]

The luminescence properties of Si nanocrystals (Si-ncs) depend strongly on the size. The high-energy shift of the photoluminescence (PL) maximum and shortening of the PL lifetime with decreasing the size have commonly been observed for different kinds of Si-ncs samples.[1,2] The PL properties are also modified by shallow impurity doping.[3–6] In general, heavy doping of either *n*- or *p*-type impurities degrades the PL properties, i.e., the PL intensity decreases due to efficient Auger recombination.[7] However, the localization of carriers by impurity doping in addition to that by the geometrical confinement may lead to further enhancement of oscillator strength of excitons in Si-ncs and thus impurity doping is a fascinating approach to improve the luminescence properties if Auger recombination can be avoided. The Auger process can be avoided if isoelectronic impurities are used. Unfortunately, Si does not have proper isoelectronic impurities that can strongly localize excitons at room temperature. An alternative approach is to use simultaneously *n*- and *p*-type impurities for doping of Si nanocrystals. The codoping and compensation of carriers may result in localization of excitons without being afraid of the Auger process.

In previous papers,[4,5] we demonstrated that P and B codoped Si-ncs show strong PL in the near infrared (IR) range at room temperature. The PL maximum depends on the doping levels as well as the size of Si-ncs. In intrinsic Si-ncs, the PL energy can be controlled only above the bulk band gap (1.12 eV). In codoped Si-ncs, the range can be extended to 0.9 eV by properly controlling *n*- and *p*-type impurities. The low energy PL is considered to arise from optical transitions between donor and acceptor states.

The strong modification of PL spectra by impurity doping indicates that the electronic structure is strongly modified. In contrast to limited number of experimental work on impurity doped Si-ncs, theoretically, studies on the electronic structure have been performed intensively.[8–14] In particular, Ossicini *et al.*[12] studied the formation energy and electronic structures of P and B codoped Si-ncs by first-principles calculations. They showed that formation energy of P and B codoped Si-ncs is much smaller than that of either P or B doped Si-ncs. Furthermore, the calculation shows that the highest occupied molecular orbital and the lowest unoccupied molecular orbital are localized around the impurity sites resulting in lowering the energy gap with respect to that of the undoped Si-nc.

The purpose of this work is to access to the electronic structures of P and B codoped Si-ncs experimentally. In a previous work,[15] we studied P-doped Si-ncs by electron spin resonance (ESR) spectroscopy. We showed that the temperature dependence of a conduction electron signal obeys Curie's law even when the doping level was very high. This suggests that in P-doped Si-ncs, donor levels do not merge into the conduction band even at very high P concentration and that Si-ncs smaller than a certain threshold size do not become metallic, at least when they are prepared under a thermal equilibrium condition. In this paper, we extend the previous work to B-doped Si-ncs and P and B codoped Si-ncs. By comparing ESR and PL data, we will show that strong localization of carriers in codoped Si-ncs is responsible for the room-temperature low-energy PL.

P and B doped Si-ncs were prepared by the same method as used in our previous work.[3–5,16] Si chips and B_2O_3 tablets were placed on a phosphosilicate glass sputtering target and they were simultaneously sputtered in Ar gas on fused-quartz or stainless steel substrates. After deposition, films were removed from the stainless steel substrates and ground to powder. The powder and films on fused-quartz substrates were then annealed in a N_2 gas atmosphere at 1150 °C for 30 min to grow P and B codoped Si-ncs in borophosphosilicate glasses (BPSG). Si-ncs are isolated each other by BPSG matrices and thus carriers are confined within Si-ncs. In this work, P concentration in films was almost fixed (1.9 at. %) while B concentration was changed from 0 to 1.36 at. %. As a reference, B doped Si-ncs was also prepared. The B concentration was changed from 0.37 to 1.51 at. %. Si concentration was fixed to about 40.5 at. % for all the samples.

X-band ESR spectra were measured for powder samples by a conventional ESR spectrometer (EMX081, Bruker) at

a)Author to whom correspondence should be addressed. Electronic mail: fujii@eedept.kobe-u.ac.jp.

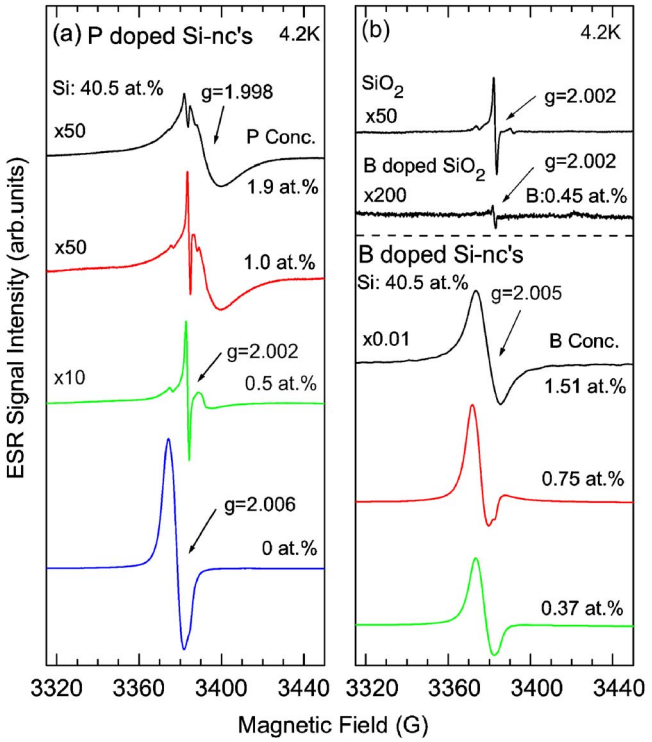

FIG. 1. (Color online) ESR spectra of (a) P doped and (b) B doped Si-ncs at 4.2 K. Si concentration is fixed at 40.5 at. %. P and B concentrations are changed from 0 to 1.9 at. % and from 0.37 to 1.51 at. %, respectively. ESR spectra of sputter-deposited SiO_2 and B doped SiO_2 are also shown as references on the upper part of (b). For better comparison, the spectra are scaled by the indicated multiplication factors.

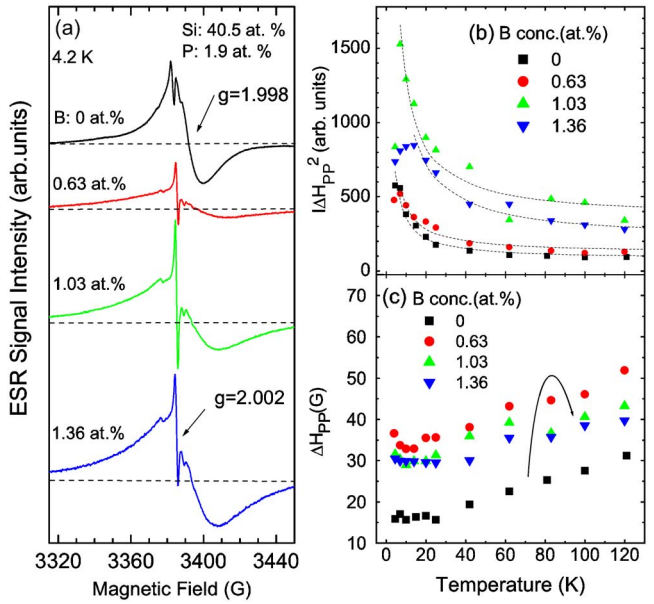

FIG. 2. (Color online) ESR spectra of P and B codoped Si-ncs at 4.2 K. Si and P concentrations are fixed at around 40.5 and 1.9 at. %, respectively. B concentration is changed from 0 to 1.36 at. %. (b) ESR signal intensity and (c) width as a function of temperature. Dotted curves in (b) are guides for the eyes.

temperatures between 4.2 and 300 K in a continuous-flow He cryostat (ESR900, Oxford Instruments). The modulation frequency and modulation amplitude were 100 kHz and 2 G, respectively. A nuclear magnetic resonance Gauss meter with 10^{-6} G resolution was used for field monitoring. The signal intensity was corrected with Mn^{2+} marker by a conventional ESR spectrometer (JES-TE300, JEOL). PL spectra were measured for film samples by using a single grating monochromator and a liquid N_2 cooled InGaAs near-IR diode array. The spectra were calibrated with the aid of a reference spectrum of a standard tungsten lamp. The excitation source was a 488 nm line of an Ar ion laser.

First, we briefly summarize ESR data of P doped Si-ncs. Figure 1(a) shows ESR spectra of P doped Si-ncs at 4.2 K. The Si concentration is 40.5 at. % and the P concentration is changed from 0 to 1.9 at. %. For better comparison, the spectra are scaled by the indicated multiplication factors. Three signals with different g values ($g=2.006$, 2.002, and 1.998) are observed. The signal with $g=2.006$ is due to dangling bond defects at $Si-SiO_2$ interfaces.[3] Although the intensity of this signal is very large, it vanishes quickly by P doping. The signal with $g=2.002$ can be assigned to an EX center characterized by involved hyperfine structure of 16 G splitting.[17] The signal is also observed for sputter-deposited pure SiO_2 [upper part of Fig. 1(b)]. The EX center becomes weaker with increasing the P concentration. At high P concentration (1.0 and 1.9 at. %), a broad signal with $g=1.998$ emerges. This signal is assigned to conduction electrons in Si-ncs.[18]

Figure 1(b) shows ESR spectra of B doped Si-ncs at 4.2 K. In contrast to P doping, the signal with $g=2.005$ due to dangling bond defects becomes strong with increasing B concentration. The different behavior of the defect density between n- and p-type doping suggests that the defects are positively charged and are deactivated by electrons supplied by P doping. Note that this signal is not observed for sputter-deposited pure SiO_2 and B-doped SiO_2 [upper part of Fig. 1(b)], and observed only when Si-ncs are grown in glasses.

In Fig. 1(b), in contrast to P doping, signals from carriers (holes) are not observed. However, it does not mean absence of holes. In general, ESR signal of holes in Si is difficult to detect because of the degeneracy of valence band maxima, and resultant very fast spin relaxation, which broaden the signal significantly. The signal can be detected by applying an external uniaxial stress.[19] Furthermore, in very high quality lightly doped crystals, random internal strains due to dislocations, imperfections, and phonons split the valence band and hole signals are observed.[20,21] In the present system, the doping level is very high and the environment of acceptors is expected to be very inhomogeneous due to the distributions of the number and sites of impurities, size, and shape of Si-ncs and strains. These inhomogeneities result in large distribution of resonant magnetic field and hole signals are considered to be too broad to be detected.

Figure 2(a) shows ESR spectra of P and B codoped Si-ncs at 4.2 K. The P concentration is fixed at 1.9 at. %, while the B concentration is changed from 0 to 1.36 at. %. As mentioned above, at the B concentration of 0 at. %, i.e., P doped samples, the broad signal is assigned to conduction electrons. The ESR intensity depends strongly on B concentration. Furthermore, the shape changes from almost symmetric at the B concentration of 0 at. % to asymmetric (Dysonian shape) at 0.63 at. %, and then becomes almost symmetric at 1.36 at. %.

In order to discuss the change of the signal shape in detail, the intensity ($I\Delta H_{PP}^2$) and the width (ΔH_{PP}), where I and ΔH_{PP} are peak-to-peak intensity and distance (width), respectively, are estimated. The EX center signal is subtracted before estimating I and ΔH_{PP}. In Figs. 2(b) and 2(c),

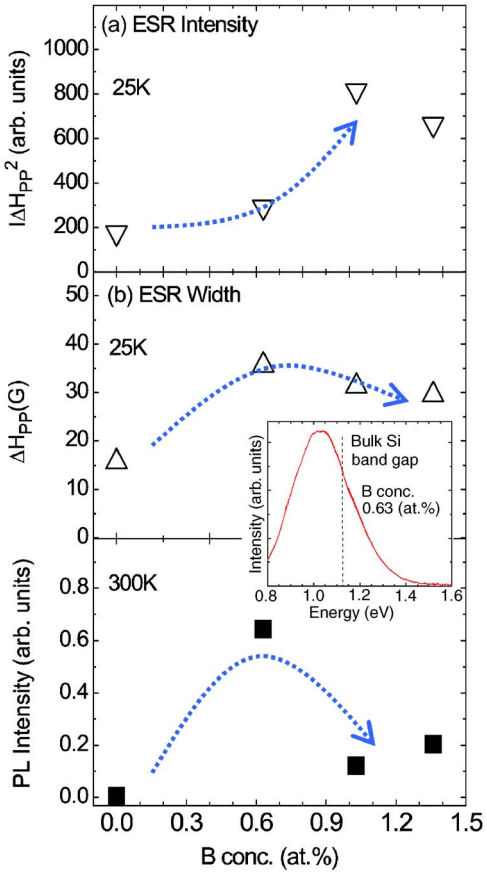

FIG. 3. (Color online) (a) ESR signal intensity ($I\Delta H_{PP}^2$), (b) width (ΔH_{PP}), and (c) PL intensity as a function of B concentration. Inset is a PL spectrum for the sample with the B concentration of 0.63 at. %.

the intensity and the width are plotted as a function of temperature. For all the samples, the intensity is nearly inversely proportional to the temperature except for a very low temperature range below 15 K. This Curie-like paramagnetism indicates that Si-ncs do not become metallic even in a heavily doped condition. The mechanism of this phenomena is discussed in our previous paper.[15] In Fig. 2(c), we can see that the signal width of codoped Si-ncs is always much larger than that of P doped Si-ncs (■).

In Figs. 3(a) and 3(b), the intensity and the width at 25 K are plotted as a function of B concentration. Similar graphs can also be obtained at other temperatures above 20 K. In Fig. 3(a), the intensity is nearly constant up to the B concentration of 0.63 at. % and increases drastically by further increasing the B concentration. On the other hand, the width shows different behavior. The width is the smallest for P doped Si-ncs, although it is several times larger than that of P doped bulk Si crystals.[15] The width increases significantly by B doping and reaches maximum when the B concentration is 0.63 at. %. Further increase in B concentration results in the decrease in the width.

The increase in the ESR intensity by B doping is mainly due to significant increase in the width. A possible mechanism of the broadening is the enhancement of interaction between confined carriers and impurities by simultaneous P and B doping. In heavily doped and compensated bulk Si crystals, broadening of ESR signals due to impurity field is reported.[22] Similarly, in codoped Si-ncs, electrons (holes) are given repulsion by negatively charged acceptors (positively charged donors) by Coulomb interaction, which results in the strong localization. The stronger localization of carriers in codoped Si-ncs than in singly doped (P-doped) Si-ncs is considered to be responsible for the significant broadening of the ESR signal.

In Fig. 3(c), PL peak intensity is plotted as a function of B concentration. When B concentration is zero, i.e., only P is doped, the PL intensity is very small due to efficient Auger process between photoexcited excitons and excess electrons. The intensity increases when B is simultaneously doped, and then decreases again when B concentration is further increased. Figure 3(c) suggests that the number of compensated Si-ncs is the largest when B concentration is 0.63 at. % within the present series of samples. In the inset of Fig. 3, PL spectrum of the sample with the highest PL intensity is shown. The PL peak energy is below the band gap energy of bulk Si crystals. By comparing Figs. 3(b) and 3(c), we can see a correlation between the ESR width and the PL intensity. This correlation suggests that carriers are strongly localized in compensated Si-ncs and the strong localization causes efficient PL at room temperature.

In higher B concentration range (1.03 and 1.36 at. %) in Fig. 3(c), the PL intensity decreases significantly and the ESR signal intensity increases abruptly [Fig. 3(a)]. This correlation suggests that PL quenching is due to nonradiative Auger process between photoexcited excitons and holes supplied by B doping. However, this is in contradiction to the data in Fig. 1(b) in which signals from holes are not detected in B doped Si nanocrystals. Probably, energy band structure of P and B codoped Si-ncs is significantly modified from that of B doped Si-ncs and the degeneracy of the valence band is lifted.

In conclusion, ESR and PL studies of P and B codoped Si-ncs indicate that in addition to geometrical confinement, further localization of carriers is possible by properly controlling *n*- and *p*-type impurities in Si-ncs. If carriers are perfectly compensated, the localization may result in the enhancement of exciton radiative recombination rate without being afraid of the nonradiative Auger process.

This work is supported by a Grant-in-Aid for Scientific Research from the MEXT, Japan, and by a grant from department of frontier research and technology, Kobe University.

[1] D. Kovalev *et al.*, Phys. Status Solidi B **215**, 871 (1999).
[2] S. Takeoka *et al.*, Phys. Rev. B **62**, 16820 (2000).
[3] M. Fujii *et al.*, J. Appl. Phys. **87**, 1855 (2000).
[4] M. Fujii *et al.*, J. Appl. Phys. **94**, 1990 (2003).
[5] M. Fujii *et al.*, Appl. Phys. Lett. **85**, 1158 (2004).
[6] X. D. Pi *et al.*, Appl. Phys. Lett. **92**, 123102 (2008).
[7] C. Delerue *et al.*, Phys. Rev. Lett. **75**, 2228 (1995).
[8] Z. Zhou *et al.*, J. Am. Chem. Soc. **125**, 15599 (2003).
[9] D. V. Melnikov and J. R. Chelikowsky, Phys. Rev. Lett. **92**, 046802 (2004).
[10] Z. Zhou *et al.*, Phys. Rev. B **71**, 245308 (2005).
[11] G. Cantele *et al.*, Phys. Rev. B **72**, 113303 (2005).
[12] S. Ossicini *et al.*, Appl. Phys. Lett. **87**, 173120 (2005).
[13] F. Iori *et al.*, Phys. Rev. B **76**, 085302 (2007).
[14] Q. Xu *et al.*, Phys. Rev. B **75**, 235304 (2007).
[15] K. Sumida *et al.*, J. Appl. Phys. **101**, 033504 (2007).
[16] M. Fujii *et al.*, Phys. Rev. Lett. **89**, 206805 (2002).
[17] A. Stesmans and F. Scheerlinck, Phys. Rev. B **51**, 4987 (1995).
[18] J. Müller *et al.*, Phys. Rev. B **60**, 11666 (1999).
[19] G. Feher *et al.*, Phys. Rev. Lett. **5**, 309 (1960).
[20] H. Neubrand, Phys. Status Solidi B **86**, 269 (1978).
[21] H. Neubrand, Phys. Status Solidi B **90**, 301 (1978).
[22] M. J. Hirsch *et al.*, Phys. Rev. Lett. **68**, 1418 (1992).